

Supplementary Material

Hollow terbium metal-organic-framework spheres: Preparation and their performance in Fe^{3+} detection

Xiaozhan Yang^{1, 2,*}, Yicun Liang¹, Wenlin Feng^{1, 2}, Chaolong Yang³, Lian Wang⁴, Guojia Huang⁵, Daoyuan Wang⁶

¹School of Science, Chongqing University of Technology, Chongqing 400054, China.

²Chongqing Key Laboratory of Green Energy Materials Technology and Systems, Chongqing 400054, China.

³School of Materials Science and Engineering, Chongqing University of Technology, Chongqing 400054, China.

⁴Guangzhou Special Pressure Equipment Inspection and Research Institute, Guangzhou 510663, China.

⁵Department of Department of Medical Research, Guangdong Provincial People's Hospital, Guangdong Academy of Medical Sciences, Guangzhou 51000, China.

⁶Department of Chmistry and Physics, University of Arkansas at Pine Bluff, AR 71601, USA.

Key words: Tb-MOFs, Hollow sphere, Luminescence, Fe^{3+} sensing

Table of Contents

Table S-1. Crystallographic data of Tb-MOFs.

Table S-2 Partial bond lengths in Tb-MOFs crystal.

Table S-3. Partial bond angles in Tb-MOFs crystal.

Table S-4. Amount of $\text{Tb}(\text{NO}_3)_3 \cdot 6\text{H}_2\text{O}$, H_3BTC and H_2TDC in the synthesis of Tb-MOFs.

Table S-5. Elemental analysis data for 1 h, 2 h, 3 h, 4 h, 6 h and 72 h during Tb-MOFs preparation.

Table S-6. Elemental data of Tb-MOFs with different $\text{H}_3\text{BTC}/\text{H}_2\text{TDC}$ ratio.

Figure S1 The Synthesis flow chart of Tb-MOFs.

Figure S2 Coordination diagram in Tb-MOFs.

Figure S3 XRD patterns of Tb-MOFs.

Figure S4 TG curves of Tb-MOFs.

Figure S5 a-g) SEM images of Tb-MOF with different $\text{H}_3\text{BTC}/\text{H}_2\text{TDC}$ ratio of (1:1, 2:1, 3:1, 4:1, 1:2, 1:3, 1:4), h) SEM image of Tb-MOF outer surface with the $\text{H}_3\text{BTC}/\text{H}_2\text{TDC}$ ratio of 1:2. (All scales are 1 μm)

Figure S6 Line scanning profiles of Tb element distribution.

Figure S7 a) Emission spectra of Tb-MOFs with different $\text{H}_3\text{BTC}/\text{H}_2\text{TDC}$ ratios, b) Excitation and c) Emission spectra of the solid-state Tb-MOF, $\text{Fe}^{3+}@\text{Tb-MOF}$ and H_3BTC , d) Emission spectrum of H_3BTC under 290 nm excitation.

Figure S8 The selectivity of Tb-MOFs to Fe ions with multiple ions exist simultaneously in aqueous.

Figure S9 The selectivity of Tb-MOFs to Fe^{3+} in DMF system.

Figure S10. a) Histogram of Tb-MOFs luminescence intensities in DMF solutions with different metal ions (at 545 nm), and the inset is emission spectra. b) Emission spectra of Tb-MOFs in various concentrations of Fe^{3+} solutions, and the inset is emission spectra near 545 nm. c) Fitting curves of luminescence intensities of Tb-MOFs versus Fe^{3+} concentrations (0-150 μM), and the inset is luminescence intensities versus low Fe^{3+} concentration (0-10 μM). d) Stern-Volmer fitting curve (Fe^{3+} concentration: 0-150 μM), and the inset is Stern-Volmer fitting curve at low Fe^{3+} concentration: 0-8 μM).

Supporting Tables

Table S-1. Crystallographic data of Tb-MOFs

Chemical formula	C ₁₅ H ₁₇ N ₂ O ₈ Tb
Formula weight	512.22
Crystal system	monoclinic
Space group	C2/c
Unit cell dimensions	
a (Å)	18.6318(8)
b (Å)	11.445(5)
c (Å)	19.7386(8)
α(°)	90
β(°)	106.504(1)
γ(°)	90
V (Å ³)	4035.7
Z	8
T (K)	193K
λ(Å)	1.34139
Dcalcd(g cm ⁻³)	1.686
μ(mm ⁻¹)	18.426
F (0 0 0)	2000
θ range (°)	3.991-54.948
Reflection collected	15934
independent reflections	5323
Goodness-of-fit (Gof)	1.076
Rint	0.0554
R1(I > 2σ(I))	0.0395
WR2(I > 2σ(I))	0.1101
ρmaxmum/ρminmum	1.504/-2.022
CCDC	2082489

Table S-2 Partial bond lengths in Tb-MOFs crystal

Tb-MOFs		
Tb01	O002	2.443(4) Å
Tb01	O003	2.330(4) Å
Tb01	O004	2.283(4) Å
Tb01	O005	2.399(4) Å
Tb01	O006	2.415(4) Å
Tb01	O007	2.379(5) Å
Tb01	O008	2.356(4) Å
Tb01	O009	2.413(4) Å

Table S-3. Partial bond angles in Tb-MOFs crystal

Tb-MOFs			
O003	Tb01	O002	124.98(13)°
O003	Tb01	O005	75.38(14)°
O003	Tb01	O006	123.36(15)°
O003	Tb01	O007	148.35(16)°
O003	Tb01	O008	78.57(16)°
O003	Tb01	O009	78.45(15)°
O004	Tb01	O002	78.95(14)°
O004	Tb01	O003	83.94(14)°
O004	Tb01	O005	93.55(17)°
O004	Tb01	O006	149.27(14)°
O004	Tb01	O007	78.56(18)°
O004	Tb01	O008	84.38(17)°
O004	Tb01	O009	156.56(14)°
O005	Tb01	O002	54.30(12)°
O005	Tb01	O006	81.73(18)°
O005	Tb01	O009	96.81(18)°
O006	Tb01	O002	73.65(14)°
O006	Tb01	C00A	75.69(16)°
O007	Tb01	O002	77.26(15)°
O007	Tb01	O005	131.47(15)°
O007	Tb01	O006	82.02(18)°
O007	Tb01	O009	109.21(19)°
O008	Tb01	O002	148.79(15)°
O008	Tb01	O005	153.94(16)°
O008	Tb01	O006	112.66(18)°
O008	Tb01	O007	73.66(17)°

Table S-4. Amount of $\text{Tb}(\text{NO}_3)_3 \cdot 6\text{H}_2\text{O}$, H_3BTC and H_2TDC in the synthesis of Tb-MOFs

$\text{Tb}(\text{NO}_3)_3 \cdot 6\text{H}_2\text{O}$	H_3BTC	H_2TDC	$\text{H}_3\text{BTC}/\text{H}_2\text{TDC}$ ratio
1 mmol, 0.453 g	1 mmol, 0.210 g	1 mmol, 0.172 g	1:1
1 mmol, 0.453 g	4/3 mmol, 0.280 g	2/3 mmol, 0.115 g	2:1
1 mmol, 0.453 g	3/2 mmol, 0.069 g	1/2 mmol, 0.086 g	3:1
1 mmol, 0.453 g	8/5 mmol, 0.336 g	2/5 mmol, 0.069 g	4:1
1 mmol, 0.453 g	2/3 mmol, 0.140 g	4/3 mmol, 0.229 g	1:2
1 mmol, 0.453 g	1/2 mmol, 0.105 g	3/2 mmol, 0.258 g	1:3
1 mmol, 0.453 g	2/5 mmol, 0.084 g	8/5 mmol, 0.275 g	1:4

Table S-5. Elemental analysis data for 1 h, 2 h, 3 h, 4 h, 6 h and 72 h during Tb-MOFs preparation.

Time	Tb (%)	C (%)	H (%)	O (%)	N (%)
1 h	32.63	35.45	3.42	37.46	1.02
2 h	33.27	35.20	3.74	25.11	2.69
3 h	19.09	30.77	3.82	42.96	3.36
4 h	37.06	35.57	1.97	21.36	4.04
6 h	32.04	35.27	3.18	24.34	5.17
72 h	31.05	35.15	3.32	25.00	5.47

Table S-6. Elemental data of Tb-MOFs with different H₃BTC/H₂TDC ratio.

H ₃ BTC/H ₂ TDC ratio	Tb (%)	C (%)	H (%)	O (%)	N (%)
1:4	30.26	36.07	2.43	26.23	5.01
1:3	32.33	35.48	2.34	25.02	4.83
1:2	31.72	35.32	3.48	24.46	5.02
1:1	31.05	35.15	3.32	25.05	5.42
2:1	32.46	34.43	3.43	24.89	4.79
3:1	31.81	36.27	3.13	24.27	4.52
4:1	32.17	34.14	3.50	25.13	5.06

Supporting Figures

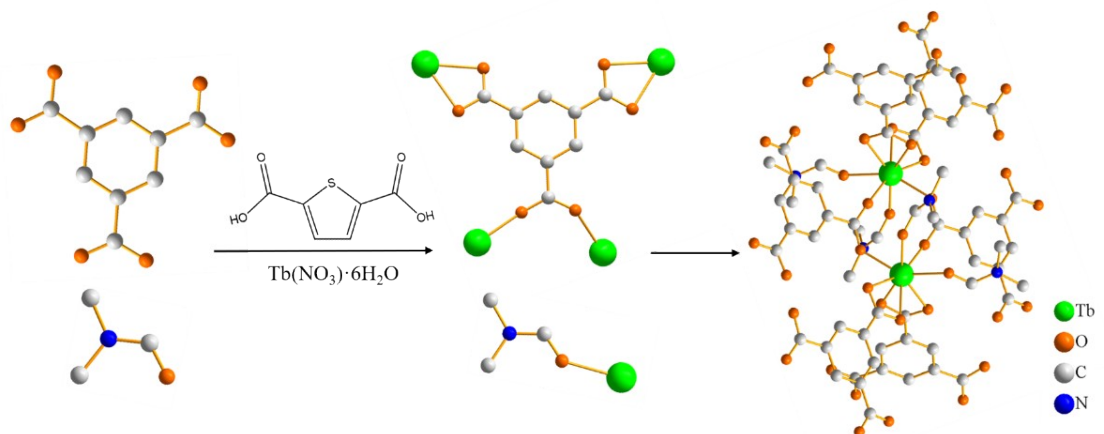


Figure S1 The Synthesis flow chart of Tb-MOFs.

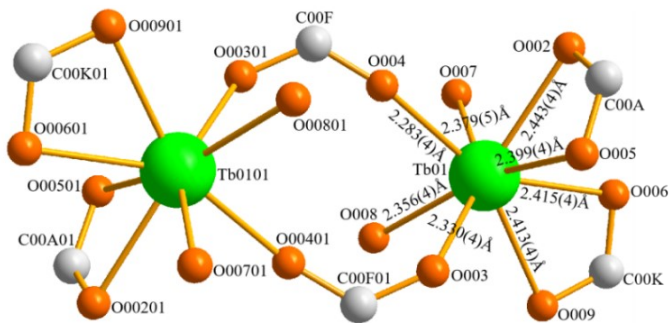


Figure S2 Coordination diagram in Tb-MOFs.

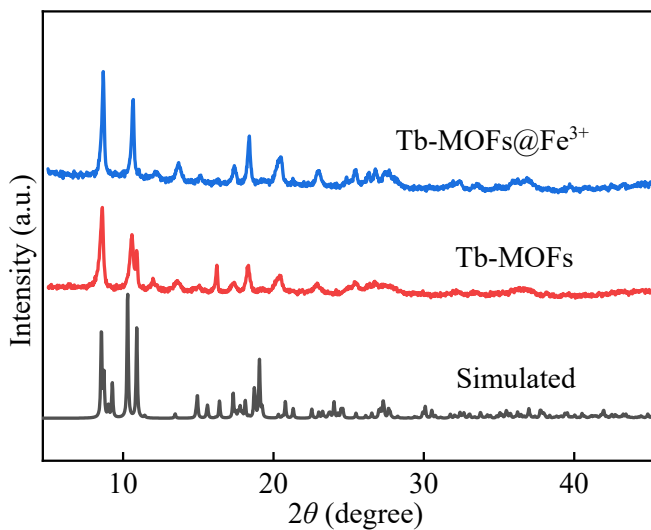


Figure S3 XRD patterns of Tb-MOFs.

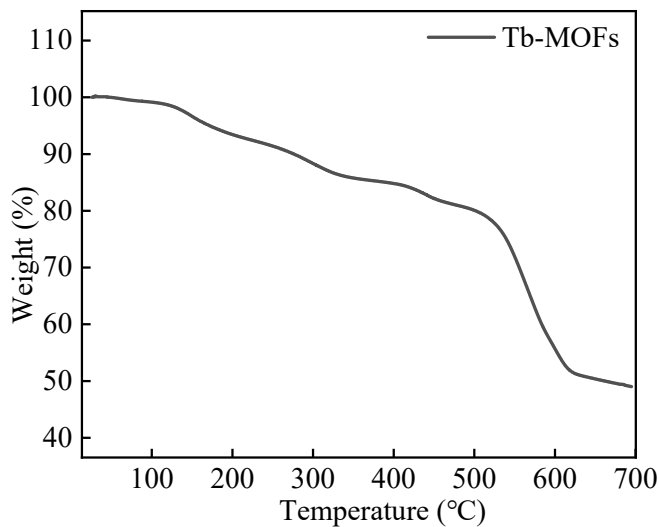


Figure S4 TG curves of Tb-MOFs.

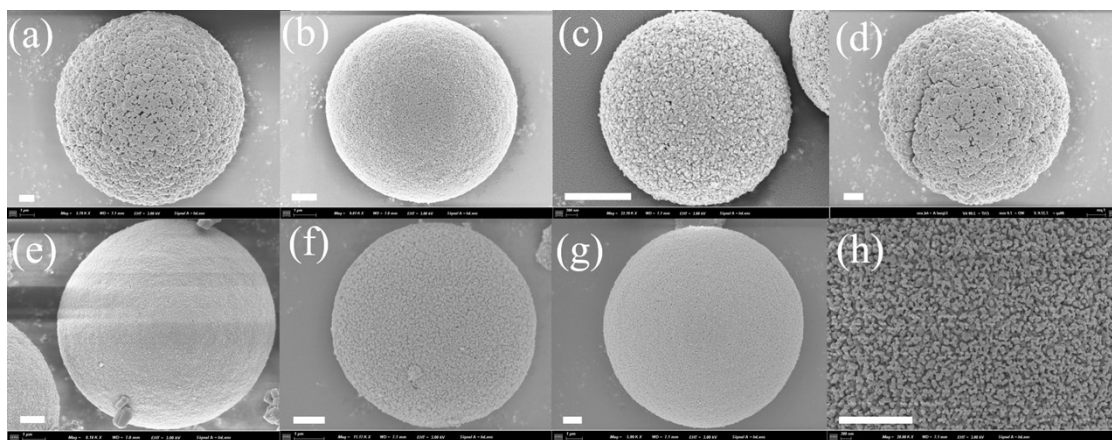


Figure S5 a-g) SEM images of Tb-MOF with different $\text{H}_3\text{BTC}/\text{H}_2\text{TDC}$ ratio of (1:1, 2:1, 3:1, 4:1, 1:2, 1:3, 1:4), h) SEM image of Tb-MOF outer surface with the $\text{H}_3\text{BTC}/\text{H}_2\text{TDC}$ ratio of 1:2. (All scales are 1 μm)

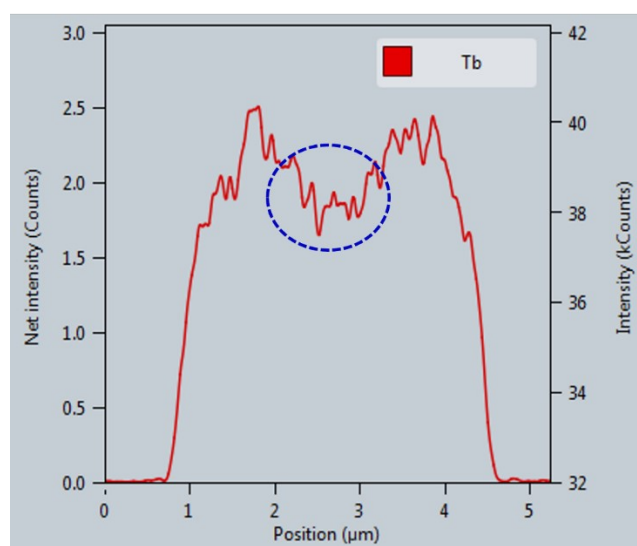


Figure S6 Line scanning profiles of Tb element distribution.

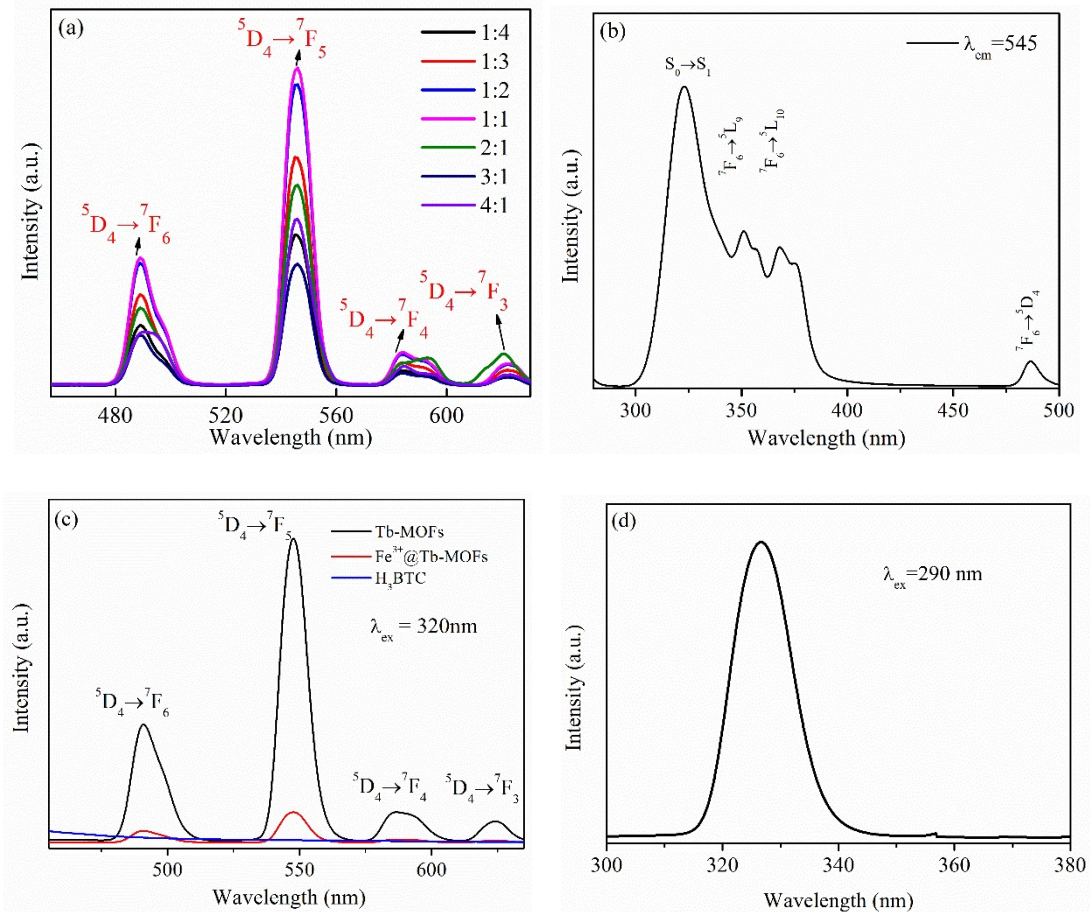


Figure S7 a) Emission spectra of Tb-MOFs with different $\text{H}_3\text{BTC}/\text{H}_2\text{TDC}$ ratios, b) Excitation and c) Emission spectra of the solid-state Tb-MOF, $\text{Fe}^{3+}@\text{Tb-MOF}$ and H_3BTC , d) Emission spectrum of H_3BTC under 290 nm excitation.

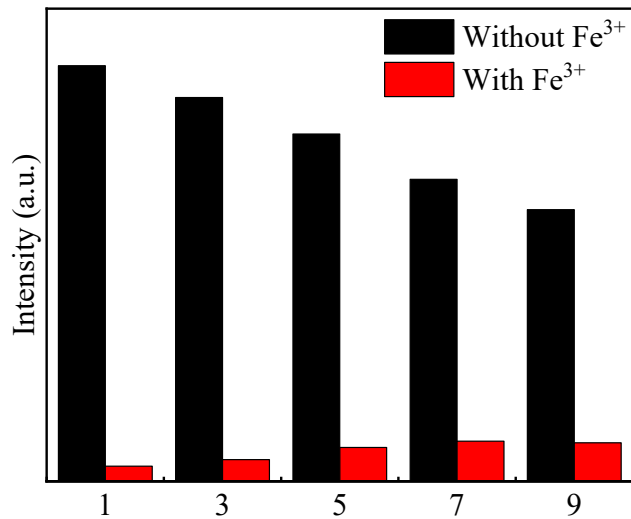


Figure S8 The selectivity of Tb-MOFs to Fe ions with multiple ions exist simultaneously in aqueous.

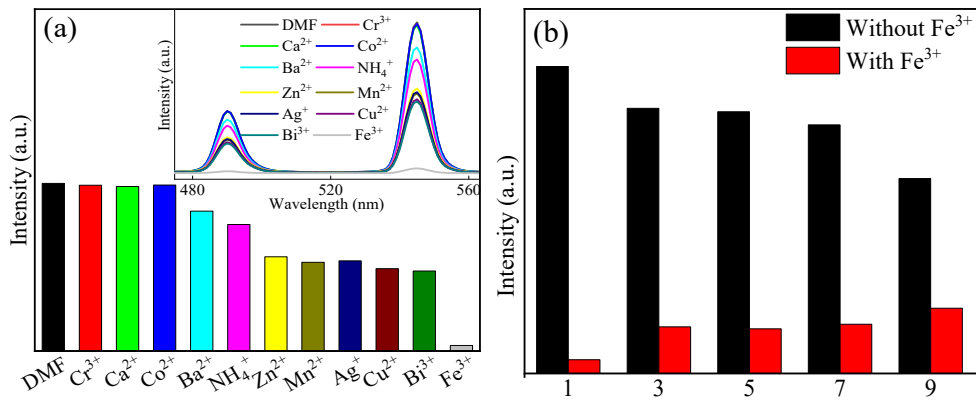


Figure S9 The selectivity of Tb-MOFs to Fe^{3+} in DMF system.

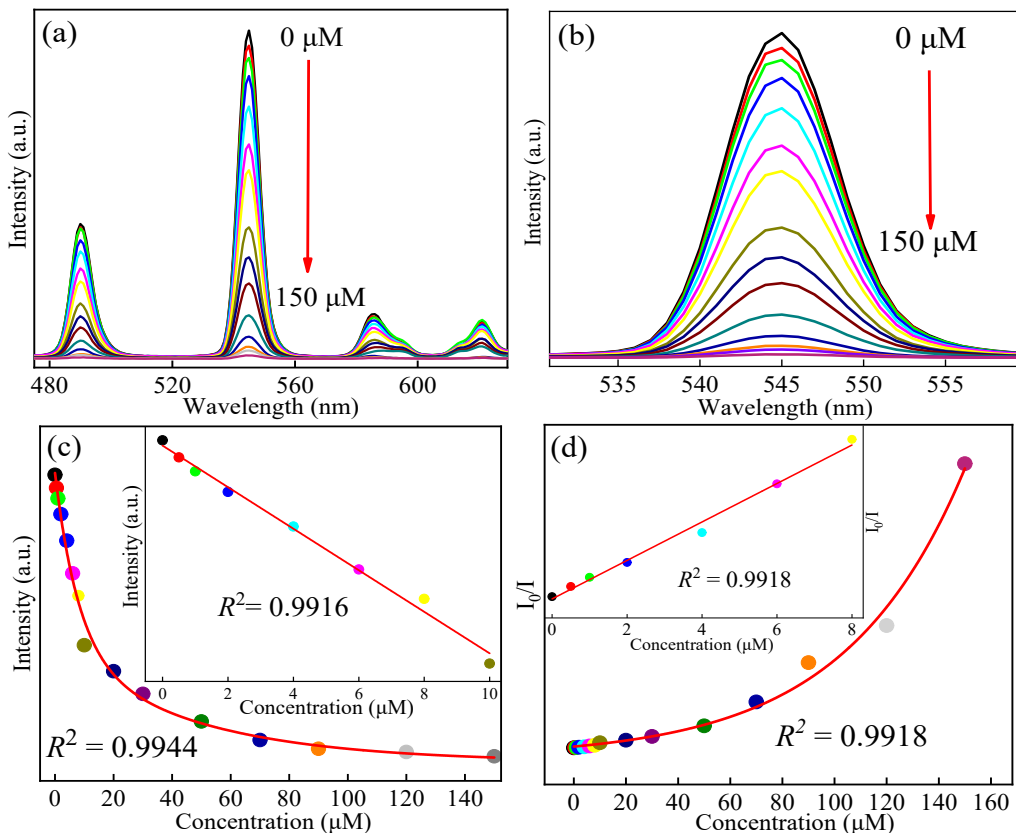


Figure S10. a) Histogram of Tb-MOFs luminescence intensities in DMF solutions with different metal ions (at 545 nm), and the inset is emission spectra. b) Emission spectra of Tb-MOFs in various concentrations of Fe^{3+} solutions, and the inset is emission spectra near 545 nm. c) Fitting curves of luminescence intensities of Tb-MOFs versus Fe^{3+} concentrations (0-150 μM), and the inset is luminescence intensities versus low Fe^{3+} concentration (0-10 μM). d) Stern-Volmer fitting curve (Fe^{3+} concentration: 0-150 μM), and the inset is Stern-Volmer fitting curve at low Fe^{3+} concentration: 0-8 μM).